Processing–Structure–Properties Relationships of Mechanically and Thermally Enhanced Smectite/Epoxy Nanocomposites

R. Kotsilkova

Bulgarian Academy of Sciences, Central Laboratory of Physico-Chemical Mechanics, Academy G. Bonchev Str., Block 1, 1113 Sofia, Bulgaria

Received 28 September 2004; accepted 24 January 2005
DOI 10.1002/app.21989
Published online in Wiley InterScience (www.interscience.wiley.com).

ABSTRACT: Mechanically reinforced and thermally enhanced smectite/epoxy nanocomposites were synthesized using "direct" (without solvent) and "solvent" processing techniques. The molecular dispersion of smectite clay in the epoxy resin was investigated for its role in the rheology, structure formation, and properties of nanocomposites. The effects of three types of organic modifiers on the dispersion structure were compared. The use of solvent during processing assists in the enhancement of clay exfoliation. Rheology was used as a method to compare the degree of clay delamination in the resin matrix, as well as to estimate the suspension structure. The critical volume fraction (Φ^*) and maximal packaging of smectites were determined and used for prediction of the viscosity. The qualitative changes in the nanostructure of suspensions above Φ^*, due to flocculation of exfoliated clay layers, were compared with the alteration of the properties of nanocomposites, related to the structure formation and morphology. The curing kinetics were found to depend on both the organic modifier and solvent, but the extent of curing was roughly equivalent for the pure epoxy resin and the nanocomposites. The structure of the nanocomposites, either intercalated or exfoliated, produced by the direct processing technique was controlled by the organic modifier. By using solvent processing, the effect of the solvent dominates that of the organic modifier, presumably leading to exfoliated nanocomposites. The mechanical and thermal properties are strongly enhanced above the Φ^* of smectites, and they are significantly dependent on the type of nanocomposite structure and the use of solvent. J Appl Polym Sci 97: 2499–2510, 2005

Key words: epoxy/smectite nanocomposites; rheology; kinetics of structure formation; mechanical properties; thermal behavior

INTRODUCTION

A number of studies have been published on the synthesis and characterization of thermosetting layered silicate hybrids.[1–6] Three types of structures are achievable by direct intercalation of the monomer into the organically modified clay galleries following *in situ* polymerization: immiscible (conventional) composites, intercalated hybrids, and delaminated (exfoliated) hybrids.[1,2] From the mechanical and barrier property standpoint, the development of exfoliated systems is preferred.[3] The vast majority of epoxy-layered silicate research has focused on epoxy-based chemistries.[1,4] These studies show that an appropriate balance between the resin intercalation within silicate galleries together with the inter- and extragallery reactions are the key factors to control the organoclay exfoliation.[6,7] According to the mechanism of clay exfoliation, as recently described by Kornmann et al.,[4] the driving force for the initial resin diffusion into the clay galleries is the high surface energy of the clay, which attracts the polar resin molecule. The efforts in nanocomposite synthesis indicate that the surface modifiers have a dominant influence on the exfoliation behavior and could act as an intragallery catalyst for amine–epoxy polymerization.[1–3]

In addition to these accomplishments, many issues associated with the generality of synthetic approaches are still unsolved. The most critical obstacles for successful commercialization of these novel materials are access to nanocomposite formulation and process technology. Substantially different materials may result in controlling the composition and processing, but a general understanding has yet to emerge. In our previous work we studied epoxy/smectite[8–10] and polypropylene/smectite[11,12] nanocomposites, which were prepared by the *in situ* polymerization method. The effects of clay exfoliation on the rheology[8] were discussed and related to the molecular dynamics[9] and thermal properties of epoxy/smectite hybrids.[10] Time-dependent viscoelastic properties in the shear and elongation flow of polypropylene/smectite hybrids were investigated[11,12] and "strain-hardening" behavior was reported. A few studies discussed the role of

Correspondence to: R. Kotsilkova (kotsil@clphchm.bas.bg).

TABLE I
Characteristics of Organosmectites

Smectite code	Name and formula of quaternized ammonium salt	ρ (g/cm^3)	Inorganic content (wt %)	d_{001} (nm)
SAN	Hexadecyl, octadecyl ammonium chloride: $[C_{16}H_{33})_{0.5}(C_{18}H_{37})_{1.5}N^+(CH_3)_2]Cl^-$	1.56	45.5	2.03
STN	Trioctane-, methyl-ammonium chloride: $[C_8H_{17})_3(CH_3)N^+]Cl^-$	1.58	69.0	2.27
SPN	Oligo(oxypropylene)-, diethyl-, methyl-ammonium chloride: $[(C_2H_5)_2(CH_3)N^+(O\text{-}iPr)_{25}]Cl^-$	1.37	35.5	4.2

ρ, specific density; inorganic content, inorganic clay in smectites determined after burning; d_{001}, XRD data of smectites from the producer and ref. 15.

processing techniques, which are necessary in ultimately fabricating thermosetting resin based nanocomposites.[5,6,13,14] Two competing considerations are discussed for the role of solvents used in the processing techniques to enhance the miscibility and processability of the initial epoxy-layered silicate mixtures. One proposes that low-boiling solvents maintain rheological properties and thus do not alter the structure or properties of the final nanocomposite.[5,6] The other considers that residual amounts of small molecule polar activators modify the interaction between the organically treated layered silicates and polymer.[13,14] Thus far, a few communications correlate the composition processing, structure, and properties of oligomer-based nanocomposites.[15,16]

The present work is focused on the relation between the rheology, structure, and mechanical and thermal properties of epoxy/smectite nanocomposites prepared by two synthesis techniques: with solvent and without solvent. The smectite/epoxy suspensions are investigated as a basic composition for synthesizing hybrids with controlled structure via subsequent curing. Rheology is used to evaluate the delamination and the structure organization of the intercalated clay layers in the molecular dispersion. The effect of both the organic modifier and the solvent on the kinetics of the structure formation is investigated and related to the reinforcement, as well as to the enhanced mechanical and thermal properties.

EXPERIMENTAL

Materials and nanocomposite preparation

Montmorillonite is a smectic clay consisting of an octahedral Al_2O_3 sheet sandwiched between two SiO_2 tetrahedral sheets, which form disks that are ~1 nm thick and have an ~50-nm radius. The charges can be adjusted by substituting Al^{3+} or Si^{4+} with Mg^{2+} and/or Fe^{2+} and the depressed charges can be neutralized with alkaline cations intercalated into the interlayer spaces, leading to a laminate structure of several hundred layers. The clay samples under study were lyophilized smectite (COOP Chemical), obtained from hydrophilic smectite intercalated with Na^+ ions by substituting them with three types of quaternized ammonium (QA) salts, denoted here as SAN, STN, and SPN. Table I presents the type of QA used and the characteristics of smectites. A low viscosity (η = 15 Pa s at 25°C) epoxy resin (Araldite LY556, Ciba) was used as the basic matrix for the smectite suspensions and diethylenetriamine was added as a curing agent for synthesizing solid composites. Toluene was chosen as a very good solvent for the organically modified smectites in the study.

The synthesis methods include two processing techniques for epoxy–smectite dispersions, denoted here as "direct" processing and "solvent" processing. In direct processing, an appropriate amount of smectites was added directly to the resin and the clay–epoxy mixture was stirred for 15 min at 500 rpm. Then, it was sonicated for 3 min using a Fisher model 300 Sonic Dismembrator (Fisher Scientific, Itasca, IL). Following sonication the samples were degased under a vacuum for 30 min at 80°C. In solvent processing, the smectite was added in toluene and the resulting dispersion was mixed with the epoxy resin. An example procedure follows. Smectite was dispersed 1:1 by weight in toluene; then the appropriate amount of epoxy resin was added, and the mixture was stirred for 15 min at 500 rpm. Toluene was subsequently evaporated under a vacuum for 30 min at 80°C. The resulting smectite/epoxy suspensions prepared by either direct or solution processing were left for 2-h cooling before rheological characterization. For preparation of nanocomposites, diethylenetriamine was added to the smectite/epoxy suspension as a hardener. Account was taken for the initiating role of the organic modifier on the epoxy curing process, when stoichiometric proportions of amine were calculated.[17,18] Samples were molded and cured by heating typically for 4 h at 80°C, followed by postcuring for 1 h at 140°C. The gel point of the curing reaction was reached after heating for

TABLE II
Rheological Characteristics of STN/Epoxy Suspensions Produced by Direct and Solvent Processing

STN content (vol %)	Direct processing $\Phi^* = 3$ vol %; $\Phi_m = 15$ vol %				Solvent processing $\Phi^* = 2.5$ vol %; $\Phi_m = 14$ vol %			
	m $(G' - \omega^m)$	G' (Pa) $\omega = 0.1$ s^{-1}	n $(\eta_{rel} \sim \dot{\gamma}^{-n})$	η_{rel} $\dot{\gamma} = 0.1$ s^{-1}	m $(G' - \omega^m)$	G' (Pa) $\omega = 0.1$ s^{-1}	n $(\eta_{rel} \sim \dot{\gamma}^{-n})$	η_{rel} $\dot{\gamma} = 0.1$ s^{-1}
0.07	2	0.004	—	1.05	1.9	0.006	0.12	1.15
1.4	0.5	0.15	0.28	1.7	0.4	0.23	0.36	7.8
3.5	0.32	1	0.43	5.2	0.28	2	0.65	54.6
11	0.15	800	0.55	65.1	0	1750	1	367.4

about 30 min at 80°C. The resulting nanocomposites were monolithic and semitransparent or transparent hybrids, depending on the processing technique. The volume fractions of the SAN, STN, and SPN smectites varied from 0.07 to 11 vol %.

Characterizations

Rheological properties of smectite suspensions in a low viscosity epoxy resin were verified by using a cone–plate viscometer (Haake RheoWin, Thermo Electron Co.) at a temperature of 20°C. The steady-state viscosity was measured in a shear rate region from 0.1 to 100 s^{-1}. Oscillatory shear mode in the frequency range of 0.01–100 s^{-1} at a low strain amplitude of 0.01% was used to measure the dynamic moduli within the linear viscoelastic range. Table II presents the most important rheological characteristics of the direct and solvent processed suspensions.

For characterization of the kinetics of structure formation, the following experiments were performed. The X-ray diffraction (XRD) spectra of samples were measured at different stages of curing by using Cu Kα radiation in the range of θ 4–24°. The IR spectra of the fully cured samples were run on Specord 75 IR spectrometer at 400–2200 cm^{-1} and at a resolution of 4 cm^{-1}. Temperature scans were taken of the cured samples by using a differential scanning calorimetry (DSC) apparatus (Perkin–Elmer DSC-7). Samples of about 1 mg were sealed in aluminum pans and heated from 0 to 300°C at a scanning rate of 10°C/min under a nitrogen atmosphere. The glass-transition temperature (T_g, midpoint) was determined from the curves using data of the second run. The data are presented in Table III. Transmission electron microscopy (TEM) micrographs were obtained on 100 nm thick samples, which were microtomed from the bulk composites by using a Phillips EM400 operating at 200 kV.

The dynamic mechanical characteristics of the solid composites [storage modulus (E'), loss modulus (E''), and tan δ] were determined on a Rheometric Scientific dynamic mechanical thermal analyzer (DMTA IV) at a strain amplitude of 0.2%, which was found to be the linear viscoelastic range for the solid epoxy composites that were studied. The cured samples were characterized in bending mode at a frequency of 1 Hz and the heating rate was controlled at 2°C/min. The measurement temperatures ranged from 23 to 300°C. The data are presented in Table III. Moreover, the mechanical properties in the bending stress–strain mode were investigated by using a Tiratest device at a speed of 2 mm/min.

The thermal behavior, thermogravimetric (TG)–derivative TG (DTG)–dynamic thermal analysis heating curves of samples were recorded with a MOM derivatograph in a temperature range of 20–1000°C at a heating rate of 5°C/min. The composite degradation was investigated in an air atmosphere without induced circulation. Table IV summarizes the results of two degradation stages: the onset temperature of decomposition (T_{onset}), determined at 5% mass loss, and the degradation temperature (T_{deg}), determined from the main peak of the DTG curves (~50% mass loss).

TABLE III
DSC and DMA Characteristics of STN Nanocomposites Produced by Direct and Solvent Processing

Sample code	T_g (°C)		T_α (°C)		tan′ δ		E'_{rel} Direct		E'_{rel} Solvent	
	Direct	Solvent	Direct	Solvent	Direct	Solvent	60°C	140°C	60°C	140°C
Epoxy	124.5	129.7	104.4	104.6	0.97	0.96	1	1	1	1
1.4 vol % STN	126.2	128.0	104.7	103.8	0.90	0.72	1.08	1.09	1.12	0.95
2.8 vol % STN	130.7	127.1	106.8	101.6	0.93	0.71	1.06	1.11	1.27	0.96
4.3 vol % STN	—	124.0	108.6	98.7	0.82	0.67	1.22	1.28	1.35	1.02

$E'_{rel} = E'_{comp}/E'_{resin}$

TABLE IV
Thermal Characteristics of Nanocomposites

Sample code	Smectite (vol %)	T_{onset} (°C)	T_{deg} (°C)
Epoxy resin	0	265	330
STN filler	—	220	580
2.5% STN	2.5	310	390
5% STN	5	320	385
10% STN	10	365	440
SAN filler	—	220	540
2.5% SAN	2.5	220	368
5% SAN	5	260	376
10% SAN	10	340	410
SPN filler	—	190	240
2.5% SPN	2.5	200	275
5% SPN	5	230	382
10% SPN	10	270	370

T_{onset}, temperature at 5% mass loss; T_{deg}, temperature at the main DTG peak (~50% mass loss).

RESULTS AND DISCUSSION

Viscous and viscoelastic properties of smectite/epoxy suspensions

Dynamic moduli were investigated at a low amplitude ($\dot{\gamma}$) of 0.01% in order to evaluate the effect of smectites on the viscoelastic properties of epoxy suspensions. Figure 1(a) presents the storage (G') and loss (G'') moduli versus the angular frequency (ω) of 5 vol % smectite/epoxy suspensions (SAN, STN, and SPN) prepared by the direct processing technique. In spite of the similar volume of inorganic content, the values of G' and G'' increase significantly in the order SAN $<$ STN $<$ SPN, thus accounting for the different miscibility of the organosmectites in the epoxy resin. Moreover, $G'(\omega)$ curves demonstrate a slope (m) in the terminal region, which is much lower than the theoretical one known for polymers. The terminal slope (m) of $G' \sim \omega^m$ curves is proposed here to quantify the degree of delamination of organosmectites in the epoxy resin. The values of (m) are 0.4 and 0.3 in SAN and STN suspensions, respectively, and even a secondary plateau is observed in the SPN suspension. Therefore, the nature and polarity of the intergallery ions of the organic modifier assist in a different way in the intercalation of epoxy molecules into the smectite gallery, resulting in an increase of the clay dispersion in the order SAN $<$ STN $<$ SPN.

Figure 1(b) compares the $G'(\omega)$ curves of STN/epoxy suspensions, prepared by both direct and solvent processing, when the volume fraction of smectite increases in the 0.07–11 vol % range. Note that the solvent processed suspensions demonstrate much higher values of G' than that of the direct processed suspensions. The terminal slope (m) of $G'(\omega)$ curves is decreased significantly by increasing the smectite content and reaches plateau values at high volume fractions. Moreover, the slope values of the solvent processed suspensions are lower than those of the direct processed suspensions at the same filler content, as shown in Figure 1(b) and Table II. Obviously, the solvent used during processing assists in the enhancement of the clay delamination in the epoxy matrix. Nonterminal behavior indicates that the relaxation of suspensions is somehow restricted in the presence of smectites. We assume that the interaction between silicate layers and the interfacial interactions lead to flocculation, which produces suppressed relaxation. The results confirm reports[19,20] that the relaxation behavior of the polymer chains is dramatically altered when they are tethered to the surface of a silicate, as in exfoliated nanocomposites, or are in close proximity to the silicate layers, as in intercalated nanocomposites.

Clay suspensions have traditionally been described as plastic flow systems, and they are expected to ex-

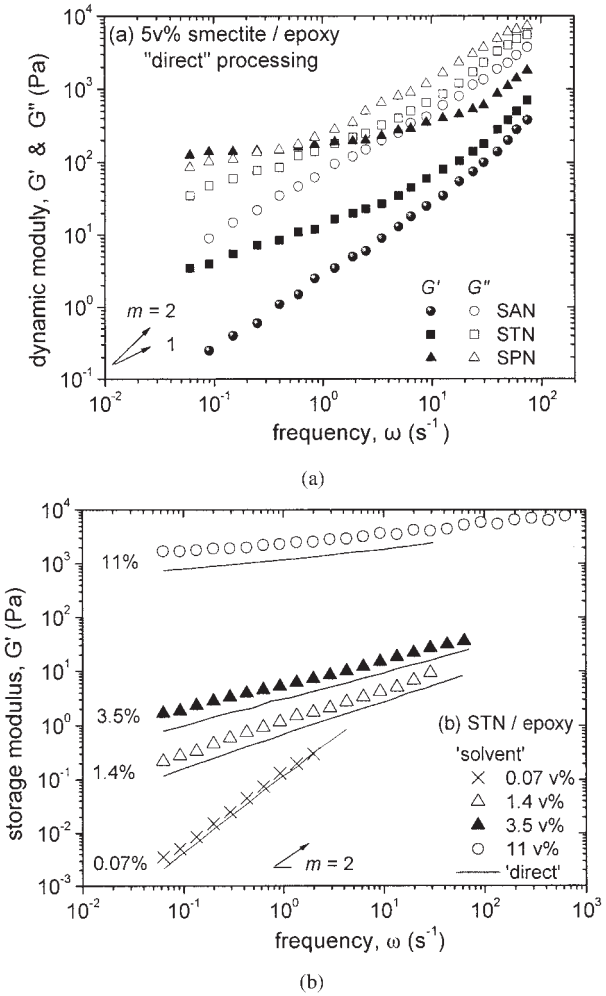

Figure 1 The low amplitude dynamic characteristics of epoxy/smectite suspensions: (a) G' and G'' versus ω of 5 vol % SAN, STN, and SPN prepared by direct processing; (b) G' versus ω of STN/epoxy suspensions, varying the volume fraction of clay. The data for solvent processing (symbols) and direct processing (lines) at 25°C are indicated; (m) is the terminal slope of $G'(\omega)$ curves.

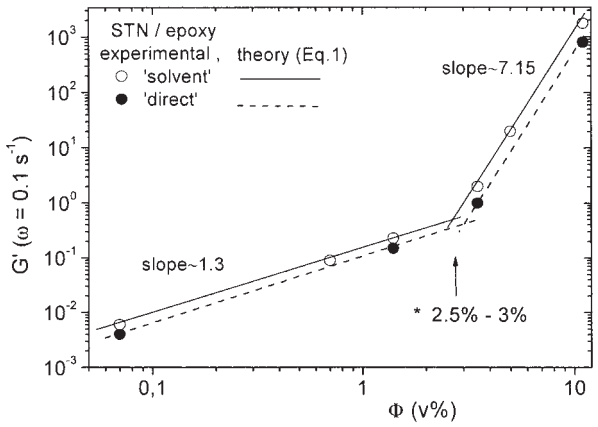

Figure 2 A log–log plot of the plateau modulus (G', at $\omega = 0.1\ s^{-1}$) versus the volume fraction of STN smectite (Φ). The arrow shows the cross point of Φ^*, that is, the critical volume fraction of flocculation; the slope values (μ) of model curves [eq. (1)] are 1.3 and 7.15 at $\Phi < \Phi^*$ and $\Phi > \Phi^*$, respectively. $\Phi^* \approx 2.5$ and 3 vol % of the solvent and the direct processed STN suspension, respectively.

hibit intriguing rheology.[15,16,19–21] However, the details are not very well understood in relation to the flow induced structure of smectites in the media.[15] In order to characterize the nature and the evolution of the structure of dispersions, we studied the effect of the smectite concentration on the viscoelastic properties. Figure 2 compares the log–log plot of the low frequency G' (at $\omega = 0.1\ s^{-1}$) versus the volume fraction (Φ) of the STN suspensions prepared by the direct and solvent processing techniques. Table II shows the data of G' at low frequency. The power law behavior of this function is usually represented by eq. (1):

$$G' \sim \Phi^{\mu} \tag{1}$$

where G' is the plateau storage modulus, Φ is the volume fraction, and μ is the exponent. The curves presented in Figure 2 have two slopes of ~1.3 at low filler contents and ~7.15 at high filler contents, respectively. The cross point has Φ^* values of 2.5 and 3 vol % for the solvent and the direct processed STN suspensions, respectively. The Φ^* value is interpreted as the critical concentration, where crowding of clay platelets appears. The observed exponent of 7.15 for the G'–Φ relationship above Φ^* is higher than most of the reported values in the literature. Many authors[21,22] have reported that the exponent for flocculated suspensions of particles is in the 2.0–5.3 range. The result of the high power in $\Phi > \Phi^*$ for smectite suspensions is indicative of a strong flocculated structure of exfoliated clay layers; thus, it seems reasonable. The clay layers in floccules are presumably ordered in stacklike multilayers, and this is reported to be associated with "edge-on-edge" interactions among the unit disks.[15,16]

To describe the suspension rheology of smectites in shear flow, for example, the viscosity η [shear rate ($\dot{\gamma}$), Φ], the flow induced flocculation/deflocculation of smectites in the epoxy resin are considered. Figure 3 gives the flow curve [relative viscosity (η_{rel}) = η/η_0 vs. $\dot{\gamma}$] for STN/epoxy suspensions prepared by both solvent and direct processing. The smectite volume fraction varies from 0.07 to 11 vol %. Here, $\eta = \eta(\dot{\gamma}, \Phi)$ is the viscosity of the suspension, and $\eta_0 = \eta(\dot{\gamma}, 0)$ is the viscosity of the matrix resin. Note that the relative viscosity is increased by increasing the smectite content, which is associated with flocculation. The suspensions demonstrate plastic behavior and the flow is highly shear thinning, accounting for deflocculation and alignment of the stacklike multilayers within the shear flow field. At smectite contents above 0.07%, the viscosity decreases gradually with increasing shear rate, which is thus more pronounced for the solution processed suspensions, assuming that the imposition of flow reduces the average size of the smectite floccules. The flow curves were fitted to the power law expression $\eta = A\ \dot{\gamma}^n$, where A is a sample specific exponential factor and (n) is the shear thinning exponent, called the index of flow. Table II presents the values of (n) for STN/epoxy suspensions, as determined from Figure 3 by a straight line fitted to the data in the low shear rate region of 0.05–1 s^{-1}. The index of flow (n) is the proposed quantitative measure of the extent of delamination of smectites, which correlates with the terminal slope (m) already obtained from the oscillatory flow experiment. We assume that both slopes (n) and (m) are dependent on the nanoscale suspension structure formed by the dispersed smectites. Rather, (n) and (m) may be used for direct comparison of the nanodispersion quality of samples prepared under different processing conditions. Both di-

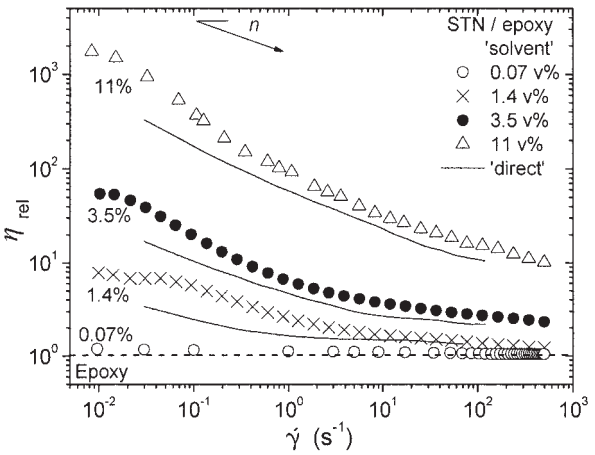

Figure 3 The relative viscosity (η_{rel}) versus the shear rate ($\dot{\gamma}$) of STN/epoxy suspensions, while varying the volume fraction of smectite. The solvent (symbols) and the direct (lines) processed systems are compared at 25°C; (n) is the shear thinning exponent (flow index).

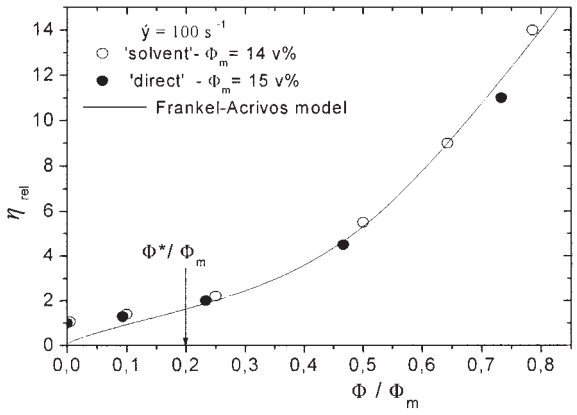

Figure 4 The relative viscosity (η_{rel}, at $\dot{\gamma}$ = 100 s^{-1}) of STN/epoxy suspensions plotted as a function of the reduced volume fraction of smectite (Φ/Φ_m). Data for the (○) solvent and (●) direct processed systems are compared. The line represents the theoretical prediction by the Frankel–Acrivos model [eq. (2)], and the arrow shows the value of Φ^*/Φ_m, that is, the limit of nanofiller leads to flocculation.

rect and solvent processing produce significant differences in the flow behavior and this may be successfully measured by (n) and (m). For example, the higher (n) and lower (m) values found in solvent processed suspensions in comparison with the direct processed one account for better delamination of STN layers with the use of toluene (Table II). Similar results are also found for SAN and SPN suspensions in epoxy resin.

The relative viscosity appears to be strongly dependent on the smectite concentration; thus, it is important to prove the applicability of the well-known theoretical predictions in order to describe the $\eta_{rel} - \Phi$ function. We have previously determined the maximal packaging (Φ_m) by using a suggestion of Thomas[23] for plotting $(\eta_{rel} - 1)^{-1}$ versus Φ, and extrapolating to zero ordinate. For example, the values of Φ_m = 14 and 15 vol % have been determined as the effective maximal packaging of the solvent and the direct processed STN suspensions, respectively. The low values of Φ_m could be explained by the nanometer thickness and very high length of the intercalated clay layers and the confined polymer molecules. Note that the values of Φ_m are shear dependent, as seen in Figure 3 from the gradually decreasing viscosity values. Thus, our calculations of Φ_m are made using the viscosity at a shear rate of 100 s^{-1}.

Based on the upper calculations of Φ_m, Figure 4 presents the reduced concentration dependence of the η_{rel} versus Φ/Φ_m, which seems to be a universal function. As shown in Figure 4, the function does not depend on the clay dispersity produced by the solvent and direct processing of STN suspensions. A number of empirical and semiempirical models are proposed in the literature to describe the concentration dependence of the viscosity. In Figure 4 we demonstrate the applicability of the Frankel–Acrivos[24] model [eq. (2)], which is proposed for colloidal dispersions to predict the rapid rise of viscosity at high concentrations, which is accounted for by the hydrodynamic interactions of neighboring spheres.

$$\eta_{rel} = \frac{9}{8} \cdot \frac{(\Phi/\Phi_m)^{1/3}}{1 - (\Phi/\Phi_m)^{1/3}} \quad (2)$$

The model prediction provided a good description of the experimental data for STN suspensions, both solvent and direct processed, when the reduced filler concentration is above $\Phi^*/\Phi_m \sim 0.2$. One can accept Φ^*/Φ_m as a limit of the filler amount that leads to flocculation of exfoliated clay layers. Further, the qualitative changes in the rheological characteristics above Φ^* are related to the changes in the suspension structure produced by the flocculation. The structure of suspensions is expected to be responsible for the alteration of the properties of nanocomposites, but only to such an extent to which the solid nanocomposite properties depend on the structure formation and morphology.

Thus, based on the rheological experiment, a method can be proposed to measure the extent of nanofiller dispersity and to evaluate the suspension structure. This method can be used as a tool for rapid control of the properties of suspensions, and it is expected to become a highly useful step in the development of nanocomposites. The method includes the following three procedures:

1. The slopes (m and n) of the rheological functions $G'(\omega)$ and $\eta(\dot{\gamma})$, respectively, are calculated and used to compare the dispersion of nanofillers in the matrix polymer.
2. The scaling of the $G'(\Phi)$ function and the scaling exponent μ, as changed at a critical concentration (Φ^*), are determined and related to the structure formation in suspensions.
3. The viscosity of systems is predicted at various volume contents of nanofiller by using theoretical models based on the maximal packaging (Φ_m) concept. This is an important technological characteristic.

Kinetics of formation of nanocomposite structure

By using XRD analyses, we have observed that the process of structure formation during curing is significantly dependent on the heating conditions, the organic modifier, and the use of solvent. Figure 5 gives evidence for the curing kinetics in nanocomposites, when controlled by the organic modifier. Thus, the diffraction spectra of the epoxy resin and 2.5% STN,

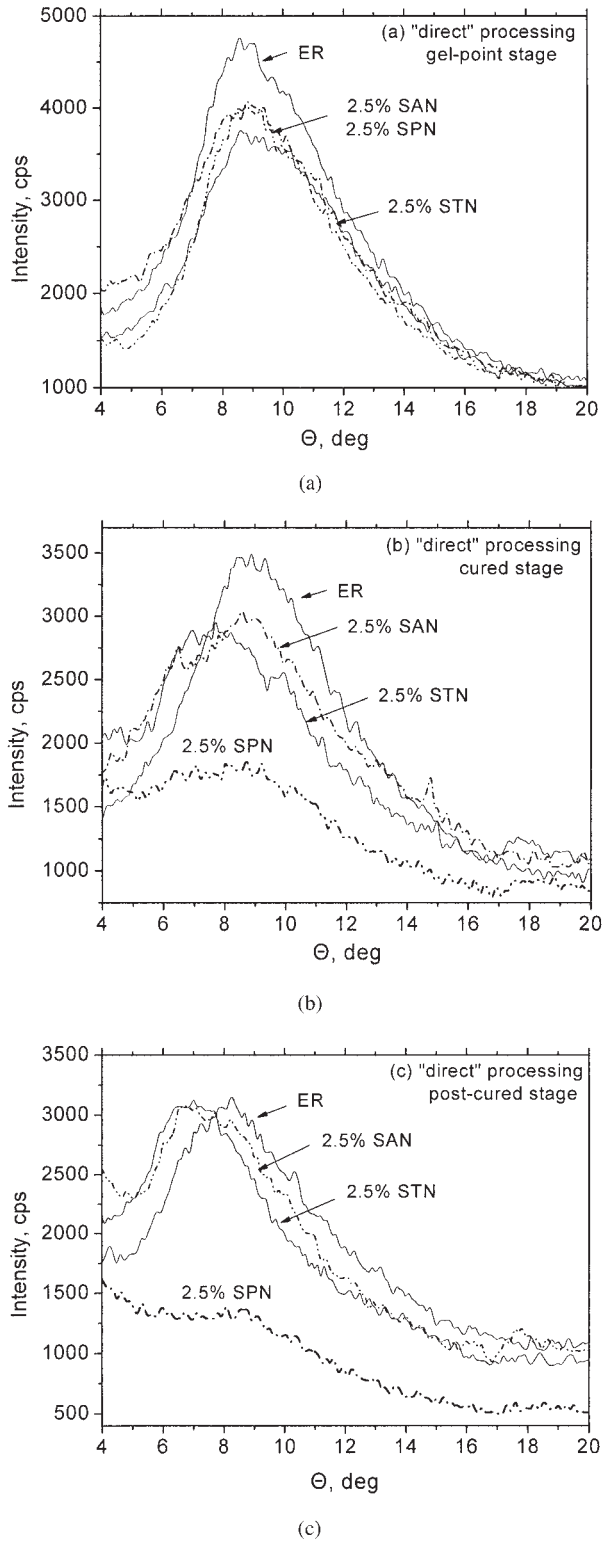

Figure 5 X-ray scattering patterns of epoxy resin and nanocomposites of 2.5 vol % SAN, STN, and SPN prepared by the direct processing technique. The curing steps are (a) gel point (30 min at 80°C), (b) cured (4 h at 80°C), and (c) postcured (1 h at 140°C) states.

SAN, and SPN nanocomposites are compared at different reaction conditions, relative to three stages of curing: gel point (30 min at 80°C), cured (4 h at 80°C), and postcured (1 h at 140°C). The diffraction range (θ 4–20°) is studied in respect to the structure of the epoxy resin.

As seen in Figure 5(a), at the gel-point stage the position of the broad basal reflection of the epoxy resin ($\theta \sim 8.5$) is not changed by the presence of SAN, STN, and SPN smectites; however, the intensity of the peak decreases in nanocomposites compared to the pure resin. This is related to the increase of the d spacing of the clay platelets, produced by the exfoliation of the clay platelets during curing until further distribution of the silicates is fixed at the gel point.[4,5] In contrast, at the cured stage [Fig. 5(b)], there is not only a decrease of intensity, but also a shift of the position of the basal reflection toward lower values, from $\theta \sim 8.5$ (epoxy resin and SAN nanocomposites) to $\theta \sim 7.4$ (STN and SPN nanocomposites), accounting for the structure formed by inter- and extragallery reactions. Finally, Figure 5(c) demonstrates the structure of the postcured samples, wherein a broad basal reflection centered on θ 8.2 is observed for the pure epoxy resin, corresponding to d spacing of 0.514 nm. However, the basal reflection of SAN and STN nanocomposites is found to be broader than that of the pure resin and the peak is shifted to lower values of θ 7.8 and 7.3, which corresponds to a gradual increase in d spacing of ~0.54 and 0.57 nm, respectively. Moreover, the SPN nanocomposite shows an absence of basal reflections in the XRD spectra. Obviously, small-scale structural domains are formed in the cured epoxy resin by the presence of smectites. Based on the results from Figure 5(c) it can be concluded that, by using a direct processing technique, both SAN and STN nanocomposites form intercalated structures whereas the SPN nanocomposite is presumably exfoliated.

Figure 6 demonstrates the structure of postcured nanocomposites when prepared by solvent processing (e.g., assisted by the use of toluene). Rheological investigations have shown that solvent processing leads to suspensions with enhanced clay delamination compared to those created by the direct processing technique. If we compare the XRD patterns of the postcured system in Figures 5(c) and 6, we observe that the structure of the pure epoxy resin is not significantly changed when it is prepared by direct or solvent processing techniques. However, the XRD spectra of SAN, STN, and SPN nanocomposites prepared by solvent processing (Fig. 6) show the absence of the basal reflection, which differs from the spectra of the direct processing from Figure 5(c). These results could be explained by the formation of an exfoliated type structure during curing for the three types of nanocomposites (SAN, STN, and SPN) when solvent processing is used.

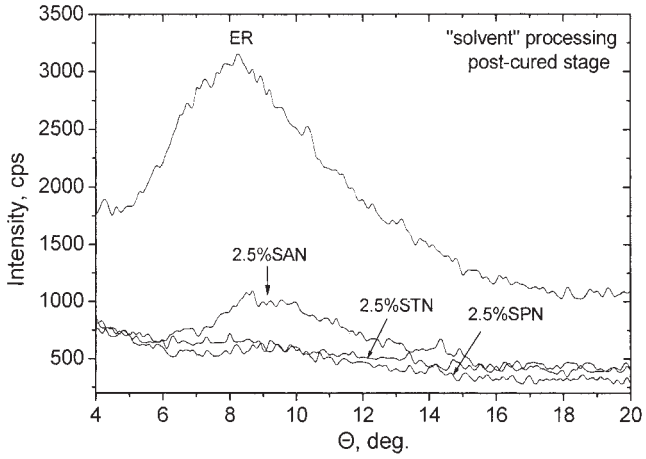

Figure 6 X-ray scattering profiles of postcured epoxy resin and nanocomposites of 2.5 vol % SAN, STN, and SPN prepared by the solvent processing technique.

This leads to the conclusion that the heating conditions during curing determine the structure formation of nanocomposites; thus, the final structure is reached at the postcured stage. The use of the solvent processing technique results in exfoliated type nanocomposites, and here the role of the organic modifier for structure formation is insufficient. In contrast, when a direct processing technique is used, the type of organic modifier controls the structure of nanocomposites during curing, resulting in either intercalated or exfoliated structures.

Curing process and morphology

The effect of various factors, such as the organic modifier, volume fraction of smectite clay, and processing conditions, on the curing process and morphology is further investigated by IR spectroscopy and TEM analyses.

Figure 7 (a,b) presents the IR spectroscopy results of postcured systems of epoxy resin and 2.5 vol % SAN, STN, and SPN nanocomposites prepared by direct processing and solvent processing techniques. The extent of curing of both types of nanocomposites is roughly equivalent to the pure epoxy resin, as given by the very low intensity of the epoxy band at 918 cm^{-1}, which indicates completely reacted epoxy groups. Interestingly, Figure 7(a) shows two novel and intensive bands that appear in the spectra of the direct processed nanocomposites (1600 and 1580 cm^{-1}), which are only slightly present in the epoxy spectra and are related to the C—N bands. The increased intensity of these bands in nanocomposites could be related to chemical bonding between the epoxy groups and the QA ions tethered at the silicate surface. The benefit of this direct attachment of the epoxy matrix to the silicate layers is in maximizing the interfacial adhesion between the two phases. In contrast, in Figure 7(b) the peaks at 1600 and 1580 cm^{-1} are only slightly present in the spectra of both the epoxy resin and solvent processed nanocomposites, which accounts for the absence of chemical bonding between the epoxy and the QA. Obviously, the residual amounts of small molecule polar solvent alter the interfacial interactions and act as a plasticizer of the epoxy resin.

The effect of the solvent on the morphology is investigated in postcured nanocomposite samples. Figure 8 compares the TEM micrographs of exemplar 5% SAN nanocomposites prepared by direct and solvent

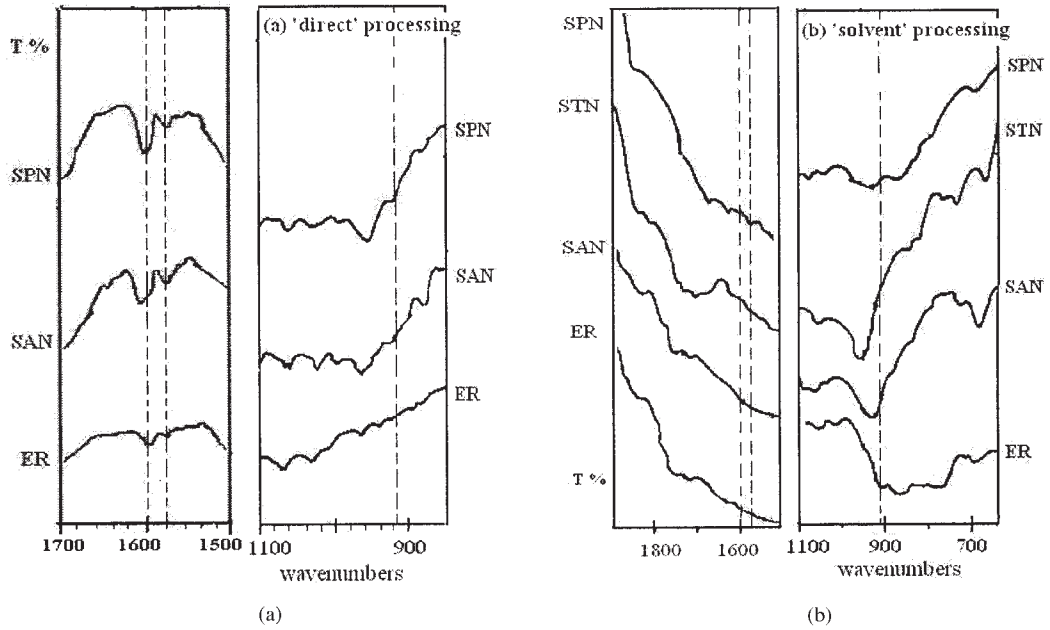

Figure 7 IR spectra of 5 vol % smectite/epoxy nanocomposites (SAN, STN, and SPN) compared to the spectrum of the pure epoxy resin: (a) direct processed and (b) solvent processed.

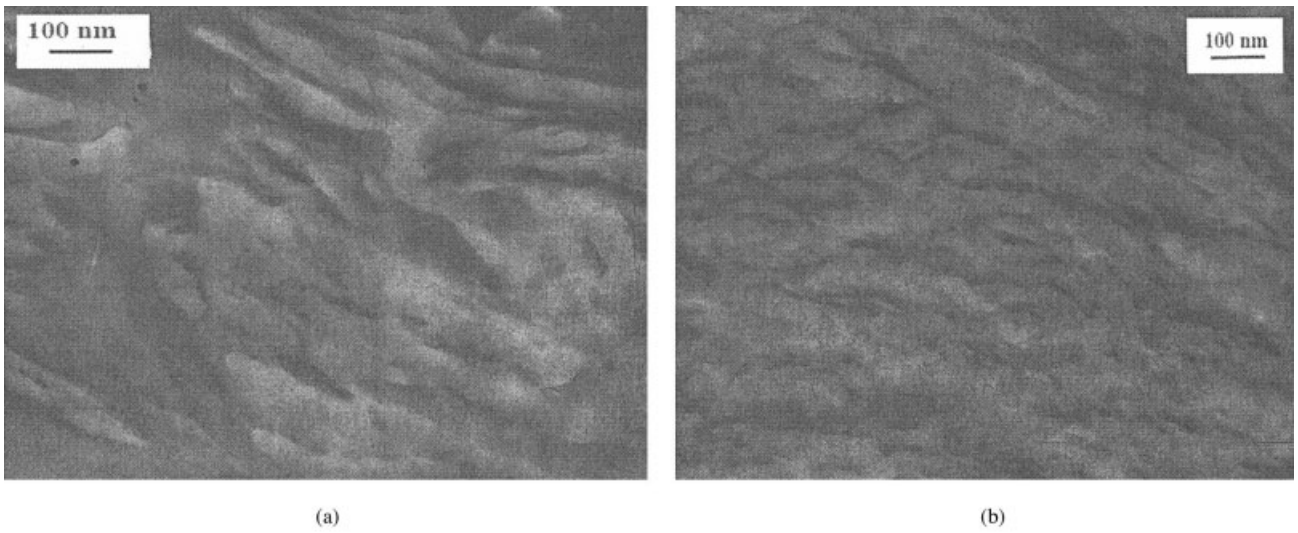

Figure 8 TEM micrographs of 5 vol % SAN nanocomposites prepared by (a) direct processing and (b) solvent processing.

processing techniques. As seen from Figure 8(a), the nanocomposite prepared by direct processing is characterized by thick stacklike smectite aggregates that are mostly oriented in one direction, which appear as dark lines with lengths of 100–500 nm and thicknesses varying from a few nanometers to 100 nm. In contrast, Figure 8(b) shows that the use of toluene in solvent processing results in the formation of much thinner stacks with improved homogeneity. These observations confirm the XRD results that the direct processing techniques produce intercalated structures whereas the solvent processing techniques presumably lead to an exfoliated structure for SAN nanocomposites. We found a similar effect of toluene on the morphology of STN and SPN nanocomposites (data not shown). The TEM results show an ordered and preferably oriented structure of smectite layers. Based on the morphological observations, we propose that the large-scale heterogeneity of the structure produced by direct processing is replaced by a small-scale heterogeneity in the solvent processed nanocomposites. This could be related to better delamination of smectites and transformation of the structure from intercalated to exfoliated with the assistance of solvent.

Reinforced mechanical properties

The reinforcement effect of nanofillers in polymers is reported as a remarkable combination of high stiffness and toughness, which is in contradiction to the conventional composites.[25–29] This synergy is probably caused by changes in the morphology of the polymer matrix because of the presence of nanofiller. There is as yet no satisfactory theoretical explanation for the origin of the improvement of the mechanical properties in polymer nanocomposites; however, it is generally agreed that the large surface to volume ratio of the nanoscale inclusions plays a significant role.

In this work we relate the mechanical properties of nanocomposites to the structure produced by clay exfoliation. Figure 9 compares the bending stress–strain curves of the epoxy resin and the 5 vol % nanocomposites of SAN, STN, and SPN. As seen in Figure 9(a), if the direct processing technique is used, about 5–15% of the increase of the bending strength is observed for nanocomposites; thus, it depends on the organic modifier. The Young's modulus (the slope of the linear initial part of bending stress–strain curves) of the nanocomposites at a fixed smectite content (e.g., 5 vol %) increases significantly in the presence of organosmectites in the following order: SPN (0%), SAN (20%), and STN (64%). However, the strain at break decreases with 15–25% for the intercalated STN and SAN systems but slightly increases for the exfoliated SPN system in comparison with that of the epoxy resin. Thus, the increased strength and brittleness of such nanocomposites can be associated with enhanced interfacial adhesion between the two phases, as well as with the large-scale heterogeneity nanostructure produced by the direct processing.

In contrast, as shown in Figure 9(b), the solvent processed nanocomposites demonstrate a significant enhancement in bending strength (30% for SAN and STN and 53% for SPN nanocomposites), accompanied with a strong increase of 50, 55, and 140%, respectively, of the strain at break. However, the Young's modulus is not changed significantly. Much stronger enhancement of the bending characteristics was found for the SPN nanocomposites because of the higher content of the paraffin-like organic modifier (SPN). In general, the increased strength and toughness of solvent processed nanocomposites can be attributed to the effect of solvent, which obviously acts as a plasti-

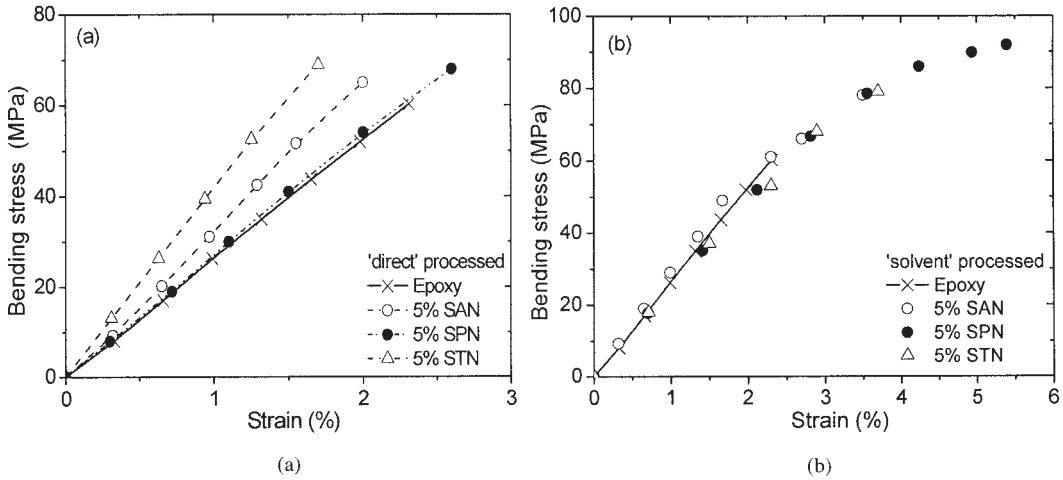

Figure 9 Bending stress–strain curves of epoxy resin and 5 vol % nanocomposites of SAN, STN, and SPN prepared by (a) direct processing and (b) solvent processing.

cizer for the epoxy resin and alters the interfacial interactions. The enhanced mechanical properties are also related to the better delamination of the smectites with the assistance of solvent, resulting in exfoliated structures with small-scale heterogeneity.

Further on we provide a more detailed definition of the role of the smectite content for the reinforcement of exfoliated nanocomposites. Dynamic mechanical thermal analyses were performed to investigate the moduli and α-relaxation (T_α), which is related to the Brownian motion of the main chains at the transition from the glassy to the rubbery state. Figure 10 compares the dynamic E' and tan δ versus the T of epoxy resin and direct processed STN/epoxy nanocomposites when varying the smectite content. Table III presents the most important dynamic mechanical data of the 1.4, 3.5, and 4.3 vol % STN nanocomposites, both direct and solvent processed, which are T_α, tan δ peak, and the relative increase of the storage modulus $E'_{rel} = E'_{comp}/E'_{resin}$ at 60 and 140°C, representing the glassy and rubbery regions, respectively. At 60°C, which is before the glass transition, the storage modulus of direct and solvent processed nanocomposites (E'_{rel}) is substantially increased by increasing the smectite loading (e.g., ~22% by direct and ~35% by solvent processed 4.3 vol % STN). The increase of the E' of nanocomposites in the glassy region in comparison with that of the epoxy matrix accounts for the reinforcement, which is produced by the presence of nanofiller. This suggests that smectites were well delaminated in the nanolayers and homogeneously dispersed in the epoxy matrix.

However, the type of processing has a different influence on the mechanical behavior of the nanocomposites around and above the glass transition (Table III). Around the glass transition, both T_α (from DMA data) and T_g (from DSC data) linearly increase in the direct processed systems when increasing the amount of

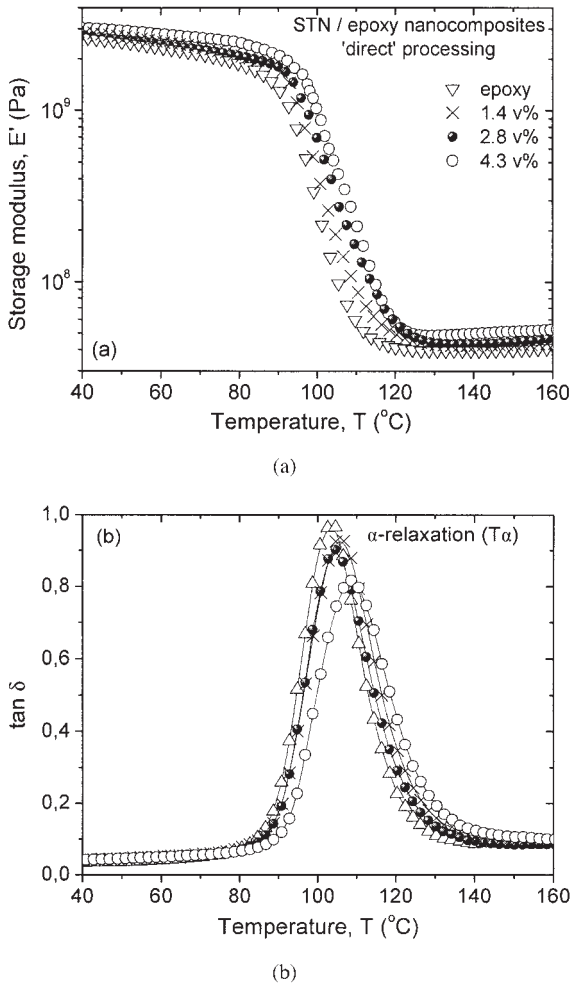

Figure 10 The dynamic mechanical characteristics versus the temperature of the epoxy resin and STN/epoxy nanocomposites prepared by direct processing: (a) storage modulus (E') and (b) tan δ, varying the smectite content. The α-transition is shown by the peak of the tan δ curves.

smectite, but they decrease in the solvent processed systems. Such behavior indicates that the restricted chain mobility of the crosslinked epoxy, which is produced by the presence of smectite, is altered with the assistance of the solvent. At temperatures above the glass transition (e.g., at 140°C), a clear increase of the storage modulus with increasing smectite content is observed in direct processed STN nanocomposites. In contrast, a slight decrease of E' is demonstrated by the solvent processed STN systems. Such observations in solvent processed nanocomposites cannot be associated with the presence of incompletely cured resin, as the results in Figure 7(a,b) indicate for completely reacted epoxy groups in all nanocomposites that were studied. One reason for such behavior could be the plasticizing effect of the residual amount of polar solvent on the epoxy resin.

The relative crosslinked density of the epoxy matrix can be estimated from the storage modulus above the glass transition temperature (in the rubbery region). Therefore, the crosslinked density of the epoxy matrix increases because of the addition of smectites in direct processed nanocomposites, thus accounting for the additional networking produced by the interfaces. However, in solvent processed nanocomposites the crosslinked density of the epoxy is slightly decreased by the assistance of solvent.

The results from Figure 10 and Table III clarify that a significant reinforcement of nanocomposites appears in the glassy region below T_g, if the volume content of smectites is above $\Phi^* \sim 2.5$–3 vol %. It is well known that conventionally prepared epoxy composites containing micron or larger sized filler particles do not exhibit substantial changes in E' at a filler volume content below 10–15 vol %.[30] We relate these observations with both the flocculated type nanostructures formed by the exfoliated clay layers and the significant effect of interfaces. Note that above Φ^*, most of the polymer is immobilized at the surfaces of the exfoliated clay layers. In direct processed nanocomposites a "bond" polymer layer is formed by a reaction of the absorbed epoxy groups with the QA modifier. The assistance of the solvent during processing enhances the exfoliation of the smectites, but it alters the interfacial interactions. As shown in our previous study,[9] the structure and molecular dynamics of the interfacial layer differ from that of the bulk polymer, and this obviously significantly dominates the overall mechanical properties of the nanocomposites above Φ^*.

Enhanced thermal properties

Recent studies are focused on improved thermal properties and flammability of polymer-layered silicate nanocomposites.[31] Our results complete these investigations in respect to the availability of smectite/epoxy nanocomposites for applications in construction materials. Here, we compare the thermal behavior of nanocomposites at a smectite loading of 2.5–10 vol % with that of the pure epoxy resin by using TG analyses (TG and DTG heating curves). Table IV presents the data from two stages of degradation of the direct processed nanocomposites by varying both the smectite content and the type of organic modifier, which are T_{onset} determined at 5% mass loss and T_{deg} at the main DTG peak (~50% mass loss). The results show that T_{onset} depends significantly on the thermal stability of the organic modifier, thus increasing in the order SPN, SAN, STN. Moreover, at a low smectite content $\Phi < \Phi^*$, the T_{onset} of nanocomposites is below or near that of pure epoxy resin. However, at $\Phi \gg \Phi^*$, the decomposition process is dominated by the presence of silicates and T_{onset} increases significantly (~75°C at 10 vol % SAN and ~100°C at 10 vol % STN). Obviously, the low mass loss of 5% at T_{onset} is associated with the water desorption and the partial degradation of the organic modifier. When the second stage of degradation (~50% mass loss) is discussed, it can be seen that the T_{deg} depends significantly on the type of nanocomposite structure. The highest effect is observed for intercalated STN and SAN nanocomposites at volume fractions above Φ^*. For example, the DTG peaks of STN nanocomposites are shifted toward higher temperatures at 55–110°C by increasing the smectite content from 2.5 to 10%, respectively. In contrast, the increase of the thermal characteristics of exfoliated SPN nanocomposites is about 40°C at 10 vol % SPN, which is obviously due to the low degradation temperature of the SPN modifier.

We propose that the enhanced thermal stability of the nanocomposites originates from the presence of smectite nanolayers, which form a specific nanostructure within the epoxy matrix. If the smectite content is above Φ^*, a large amount of the polymer is associated with the surface of the silicate nanolayers, which have a lower thermal conductivity than that of the matrix polymer. Such a structure strongly prevents any diffusion processes; it acts as an excellent insulator and mass transport barrier for the volatile products generated as the epoxy resin and QA ions degrade.

In general, the controlled increase (about 100°C) of the onset of decomposition at 5% mass loss (Table IV), as well as the significant enhancement of the mechanical characteristics (Young's modulus, bending strength, and E') in the temperature range of 20–100°C (Table III, Fig. 9) allow us to conclude that the smectite/epoxy nanocomposites could be very attractive as novel materials for construction applications.

CONCLUSIONS

Epoxy nanocomposites based on three types of organosmectites were investigated and two synthesis techniques were compared: solvent processing and direct processing (without solvent). The clay delamination in epoxy resin was found to significantly depend on the type of organic modifier, and it was

enhanced by the use of solvent. The relaxation of suspensions was somehow restricted above a critical volume fraction of nanofiller (Φ^*) and scaling of rheological characteristics appeared, which is indicative of a strong flocculated structure of smectite layers. Based on rheological experiments, a method was proposed to measure the extent of nanofiller dispersion and to evaluate the suspension structure. This method ensures rapid control of the properties of the initial suspensions, and it can be used as a highly useful tool in the development of nanocomposites.

The qualitative change in the structure of suspensions above Φ^* was compared with the alteration of the properties of nanocomposites, depending on the curing kinetics and morphology. The structure formation during curing was controlled by an organic modifier and a solvent. With the assistance of the solvent during processing, exfoliated type nanocomposites were produced and here the role of the organic modifier for the structure formation was insufficient. In contrast, when nanocomposites were prepared by direct processing, the type of organic modifier controlled the structure formation. The extent of curing was roughly equivalent for the pure epoxy resin and the nanocomposites. However, the chemical bonding between the epoxy groups and the organic modifier tethered at the silicate surfaces, as well as the overall morphology, were changed by the solvent.

The mechanical properties of nanocomposites are related to the structure and morphology. Direct processing produces mostly intercalated nanocomposites with a large-scale heterogeneity and strong interfacial bonding, which result in increased strength and brittleness. The solvent assists in better delamination of the smectites in the matrix and acts as a plasticizer for the epoxy resin. Thus, solvent processing leads to exfoliated nanocomposites with small-scale heterogeneity and altered interfacial interactions, which results in a significant enhancement of the strength and toughness. A significant reinforcement of nanocomposites appears in the glassy region if the volume content of smectites is above Φ^*.

Smectite loading strongly improves the thermal stability of epoxy nanocomposites. The onset of decomposition (5% mass loss) and the temperature of degradation (50% mass loss) are shifted ($\sim$100°C) toward higher temperatures. This effect has a significant dependence on the thermal stability of the organic modifier and the volume fraction of smectites. The highest thermal stability is observed above Φ^*, where the decomposition process is dominated by the presence of silicates having lower thermal conductivity, and a great amount of the polymer is associated with the silicate surfaces. Such nanostructures strongly prevent any diffusion processes and act as excellent insulators and mass transport barriers.

The significant and controlled increase of the thermal stability, as well as the strong enhancement of the mechanical characteristics in the 20–100°C temperature range, allow me to propose that the smectite/epoxy nanocomposites could be a lightweight and very attractive material for construction applications.

The author thanks Prof. K. Koyama and Assoc. Prof. T. Takahashi for helpful discussions during a visit to VBL, Yamagata University, Japan.

References

1. Pinnavaia, T. J.; Ian, T.; Wang, Z.; Shi, H.; Kaviratna, P. D. In Nanotechnology. Molecularly Designed Materials; Chow, G. M.; Gonsalves, K. E., Eds.; ASC Symposium Series 622; American Chemical Society: Washington, DC, 1996; p 250.
2. Vaia, R.; Jandt, K.; Kramer, E.; Giannelis, E. Macromolecules 1995, 28, 8180.
3. Wang, M.; Pinnavaia, T. Chem Mater 1994, 6, 2216.
4. Kornmann, X.; Linberg, H.; Berglund, L. Polymer 2001, 42, 1304.
5. Becker, O.; Russel, V.; Simon, G. Polymer 2002, 43, 4365.
6. Messersmit, Ph.; Giannelis, E. Chem Mater 1994, 6, 1719.
7. Bharadwaj, R.; Mehrabi, A.; Hamilton, C.; Trujillo, C.; Murga, M.; Fan, R.; Chavira, A.; Tompson, A. Polymer 2002, 43, 3699.
8. Kotsilkova, R. In Proceedings of the 13th International Congress on Rheology; Binding, D. M.; Hudson, N. E.; Mewis, J.; Piau, J.-M.; Patrie, C. J. S.; Townsend, P.; Wagner, M. H.; Walters, K., Eds.; Cambridge, UK; 2000; Vol. 4, p 145.
9. Kanapitsas, A.; Pissis, P.; Kotsilkova, R. J Non-Crystal Solids 2002, 305, 204.
10. Kotsilkova, R.; Petkova, V.; Pelovski, J. J Therm Anal Calorim 2001, 64, 591.
11. Kotsilkova, R.; Okamoto, M.; Taguchi, H.; Sato, N.; Sato, H.; Kotaka, T. In Progress and Trends in Rheology; Emri, I.; Cvelbar, R., Eds.; Steinkopf: Darmstadt, 1998; Vol. V, p 398.
12. Kotsilkova, R. Mechanics of Time Dependent Materials; Kluwer Academic: New York, 2002; Vol. 6, p 283.
13. Burnside, S.; Giannelis, E. Chem Mater 1995, 7, 1597.
14. Kemnetz, S.; Still, A.; Cody, C.; Schwindt, R. J Coating Technol 1989, 61, 47.
15. Kotaka, T.; Taguchi, H.; Sato, H.; Okamoto, M. In Proceedings of the 8th International Conference on the Mechanics and Technology of Composite Materials; Acad Pub Marin Drinov: Sofia, Bulgaria, 1997; p 285.
16. Brandenburg, U.; Lagaly, G. Appl Clay Sci 1988, 3, 263.
17. Park, J.; Jana, C. Macromolecules 2003, 36, 8391.
18. Park, J.; Jana, S. Polymer 2004, 45, 2673.
19. Krishnamoorti, R.; Vaia, R.; Giannelis, E. Chem Mater 1996, 8, 1728.
20. Krishnamoorti, R.; Giannelis, E. Macromolecules 1997, 30, 4097.
21. Gabriel, J.; Sanchez, C.; Davidson, P. J Phys Chem 1996, 100, 11139.
22. Buscall, R.; Mills, P.; Coogwin, J.; Lawson, D. J Chem Soc Faraday Trans 1988, 84, 4249.
23. Thomas, D. G. J Colloid Sci 1965, 20, 267.
24. Frankel, N. A.; Acrivos, A. D. Chem Eng Sci 1967, 22, 847.
25. Kim, G.; Lee, D.; Hoffmann, B.; Kressler, J.; Stöppelmann, G. Polymer 2001, 42, 10095.
26. Friedrich, K.; Karson, U. Fibre Sci Technol 1983, 18, 34.
27. Nicolopian, S.; Friedman, M.; Stalnova, U.; Popov, V. Adv Polym Sci 1990, 96, 1.
28. Friedrich, Ch.; Scheuchenpflug, W.; Neuhäusler, S.; Rösch, J. J Appl Polym Sci 1995, 57, 499.
29. Reynaud, E.; Jouen, T.; Gauthier, C.; Vigier, G.; Varlet, J. Polymer 2001, 42, 8759.
30. Isida, H. Controlled Interphases in Composite Materials; Elsevier: New York, 1990.
31. Gilman, J. W.; Kashiwagi, T.; Nyden, M.; Brown, J. E. T.; Jackson, C. L.; Lomakin, S.; Giannelis, E. P.; Manias, E. In Chemistry and Technology of Polymer Additives; Malaka, S.; Golovoy, A.; Wilkie, C. A., Eds.; Blackwell Science: London, 1999; p 249.